Journal of Metals, Materials and Minerals, Vol. 32, No. 1, pp. 101-108, 2022

Study of the effect of pH, conditioning and flotation time on the flotation efficiency of phosphate ores by a soybean oil collector

Zohra FARID[1], Mohamed ABDENNOURI[1], Noureddine BARKA[1], Youness JANNANI[1], and M'hamed SADIQ[1,*]

[1] *Sultan Moulay Slimane University of Beni Mellal, Research Group in Environmental Sciences and Applied Materials (SEMA), FP Khouribga, B.P. 145, 25000, Morocco*

*Corresponding author e-mail: m.sadiq@usms.ma

Received date:
20 July 2021
Revised date
1 January 2022
Accepted date:
31 January 2022

Keywords:
Phosphate ore;
Bio-flotation;
Soybean oil collector;
Gangue

Abstract

The mid-low grade of phosphate ore, rich by the silicate and carbonate gangue minerals needs a special treatment using the flotation process. Where the collectors play a pivotal role. This study was conducted to enrich an untreated phosphate ore (without washing, desliming, hydrocycling, etc.), with an eco-friendly and economic collector based on soybean oil. Different analytical techniques such as UV-Visible, ATR-FTIR spectrometric and XRD were used in order to analyse and characterize the flotation products. The effects of the parameters, pulp pH, conditioning time and flotation time on gangue removal efficiency by flotation, were investigated. Flotation tests were applied for granulometric class (90 µm to 125 µm). Consequently, a good quality phosphate concentrate was obtained in an acidic medium (pH = 4.05) with 1 g of soybean oil soap collector, 20 min flotation time, 10 min conditioning time, 0.17 $L \cdot min^{-1}$ air superficial velocity, 800 rpm at 25°C and 6% solid content. The concentrate contained 29.0% phosphorus pentoxide (P_2O_5), with a recovery of 94.5% from a feed sample containing about 24.5% P_2O_5.

1. Introduction

Phosphate is the main natural source of phosphorus [1], an element that provides a quarter of all the nutrients plants need for growth and development. The element phosphorus is one of the main constituents of reagents for the manufacture of various fertilizers, detergents, animal feeds, and other phosphorus-based chemicals such as pesticides [2]. More than 75% of the world's phosphate rock resources are distributed in the form of sedimentary deposits [3]. In the midst of these, most of these sediments have a cryptocrystalline structure, i.e., they are classified as medium to low grade phosphates, and they found side by side with quartz, calcite and dolomite as the main phases of silicate and carbonate gangues, consequently have a poor treatment. To enrich these phosphate ores various techniques are used such as calcination, fragmentation, granulometric separations, and others. Among them, froth flotation is one of the most used processes for the enrichment of sedimentary phosphate ore [4]. Sulphuric or phosphoric acid was used as a pH regulator and depressant to remove carbonate gangues from natural crude phosphate by an effective reverse flotation protocol [5,6]. Therefore, the search for better collectors to achieve perfect efficiency of phosphate flotation while respecting the environment is an important research topic. For this purpose, most of the vegetable oils studied in the previous research, are economical and ecological collectors used in froth flotation. Sesame oil [7], palm and canola oils [8], jojoba oil [9] and cottonseed oil [10] are some of these vegetable oils, which are all used in the flotation process. Soybean oil has the particularity of being rich in linoleic acid and oleic acid which they are unsaturated fatty acids. The saturated fatty acids were found to be very poor collectors when using the standard conditioning procedure, while the C16 to C22 unsaturated fatty acids showed a fair to good phosphate collection capacity [11].

In the present work, attention was paid to a very economical-ecological technique for this type of ore by flotation. It is based on the flotation of gangue minerals by a natural collector without any depression of the apatite and investigates the potential application of soybean oil soap as an alternative collector. Many parameters influence P_2O_5 flotation recovery rate and grade including pH, conditioning, and flotation time. The results obtained were confirmed by chemical and mineralogical analyses of the flotation products.

2. Materials and methods

2.1 Particle size distribution of sample

A representative sample of phosphate ore was collected from Khouribga region, Morocco. This sample was subjected to particle size distribution by the mechanical sieving method. The principle of this method is to classify the different fractions of the sample using a series of sieves. As shown in Figure 1, the variation in weight yield as a function of the granulometric ranges obtained by sieving is characterized by three classes. The main class represented by the 125 µm to 180 µm mesh size, equal to 31.5% by weight, showed higher

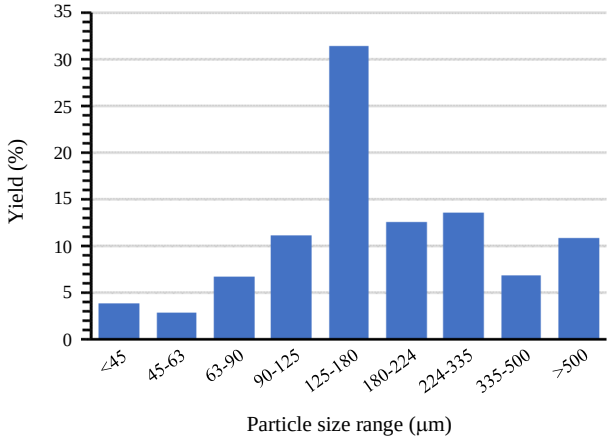

Figure 1. Yield of crude phosphate as a function of particle size.

ownability compared to other size range. The weight yield of the second series 224 µm to 335 µm, 180 µm to 224 µm, 90 µm to 125 µm, >500 µm and 335 µm to 500 µm is about 13.6%, 12.6%, 11.2%; 10.8% and 6.8% respectively; the third class represents the range of fine particle 90 µm to 63, <45 µm, and 63 µm to 45 µm with yields of 6.8%, 3.9%, and 2.8%, respectively.

2.2 Mineral composition as a function particle size

Table 1 groups the phosphorus pentoxide (% P_2O_5) analyses and the content of bone phosphate of lime (% BPL) of rock phosphate. It was found that the P_2O_5 percent was distributed almost uniformly in the different particle size fractions, rather than being enriched in particular fractions. Indeed, the P_2O_5 grade increases with increasing particle size until the fraction 125 µm to 180 µm get a higher percentage.

2.3 Flotation reagents and oil saponification

Sodium hydroxide (NaOH, 0.1 N) and phosphoric acid (H_3PO_4, 1 N) solutions were used as pH regulators. Collector based on crude soybean oil; its saponification index equal to Is = 187.45 which is determined experimentally by titration of excess sodium hydroxide with standard hydrochloric acid. Soybean oil was saponified with a standard aqueous solution of 0.5 N sodium hydroxide before being used as a collector for the flotation experiments of this study. The saponification method used consists hydrolysis of ester in basic medium, which causes the oil to transform into soap (carboxylate salt). The amount of sodium hydroxide and water was calculated according to procedure described by Abouel-enein *et al*. [7]. To make 100 g of soybean oil soap, a mass of 13.5 g of sodium hydroxide (NaOH) was dissolved in 40 mL of water and ethanol, whose alcohol present 25%, for making the two phases miscible, then mixed all these reagents under reflux heating for 40 min. Table 2 represents the different fatty acids, their chemical structure and composition that constitute soybean oil adopted by Clemente *et al*. [12]. It is composed of five fatty acids: stearic acid (18:0), linoleic acid (18:2) oleic acid (18:1), linolenic acid (18:3) and palmitic acid (16:0). The percentage of these fatty acids in soybean oil is 4%, 55%, 18%, 13%, and 10% respectively. With the exception of soybean oil, the reagents used were of high analytical quality.

Table 1. P_2O_5 and BPL composition as a function particle size.

Particle size fraction (µm)	BPL (%)	P_2O_5 (%)
<45	38.3	17.5
45-63	40.5	18.5
63-90	46.8	21.4
90-125	52.3	23.9
125-180	64.4	29.5
180-224	59.7	27.3

Table 2. Chemical composition of saturated and unsaturated fatty acids from soybean oil.

Fatty acid	Structure	Composition (%)
Stearic	$CH_3(–CH_2)_{16}–COOH$	4.0
Palmitic	$CH_3(–CH_2)_{14}–COOH$	10.0
Linolenic	$CH_3(–CH_2–CH=CH)_3(–CH_2)_7–COOH$	13.0
Oleic	$CH_3(–CH_2)_7–CH=CH(–CH_2)_7–COOH$	18.0
Linoleic	$CH_3(–CH_2)_3(–CH_2–CH=CH)_2(–CH_2)_7–COOH$	55.0

2.4 Flotation experiments

Before starting the flotation tests, the raw phosphate samples were crushed and passed through a 90 µm to125 µm mesh sieve. The flotation experiments of the naturel phosphate were performed in a cylindrical cell with a capacity of 100 mL where the pulp density was set at 6% (% solid). The phosphate minerals were conditioned to a desired pH value of 4.0, 5.5, 7.0, 8.6, and 10.0 under constant agitation at 800 rpm for 5 min, 10 min, and 20 min. Finally, the flotation tests were carried out using air at a flow rate of 0.17 L min^{-1} for various times 10 min, 20 min, 30 min, and 40 min. Both flotation resulting party (concentrate and tailings) were collected then filtered, dried, and weighed.

The grade (% P_2O_5) and recovery rate (% Re) of the valuable minerals have been calculated by the Equations (1) and (2), respectively:

$$\%P_2O_5 = \frac{\%BPL}{2.185} \quad (1)$$

$$\%Re = \frac{\%yield * \%P_2O_5(concentrate)}{\%P_2O_5(brut)} \quad (2)$$

2.5 Characterization techniques

Powder X-ray diffraction (XRD) measurements were recorded on a D2 PHASER diffractometer using CuK_α (λ=1.5406 Å) radiation. The patterns were recorded with a step of 0.02° using a counting time 0.5 s per step over the 2θ range from 10 to 80° at room temperature.

Diffuse reflectance infrared spectra for the synthesized solids were recorded from 4000 cm^{-1} to 400 cm^{-1} on a Perkin Elmer (FTIR-2000) spectrometer. Samples were prepared by mixing 1 mg of powdered solid with 100 mg of KBr. The oil spectrum was recorded after installation of a single reflection attenuated total reflectance-infrared spectroscopy (ATR) accessory. A TOMOS V-1100 UV-Vis spectrophotometer was used to determine the BPL content from its UV–Vis absorbance characteristic with the calibration curve method at the maximum absorption wavelength at 430 nm.

3. Results and discussions

3.1 Attenuated total reflectance-Infrared spectroscopy of soybean oil

Figure 2 shows the ATR-FTIR spectrum of soybean oil, various bands can be identified in this spectrum including the strong absorption band at 1742 cm^{-1} corresponds to the ester carbonyl (C=O) stretching mode. The absorption bands located at 2853 cm^{-1} and 2922 cm^{-1} are due to the symmetric and asymmetric stretching vibrations of -C-H (CH_2) and those located at 2947 cm^{-1} and 3008 cm^{-1} are due to the asymmetric stretching vibrations of -C-H (CH_3) and =C-H, respectively [13,14]. Others bands were observed at 1456 cm^{-1} and 1375 cm^{-1} that were attributed to the CH_2 and CH_3 scissoring vibrations respectively, as well as medium C–O stretching bands at 1154 cm^{-1} and 1098 cm^{-1}. According to authors [14], a weak peak observed at 1652 cm^{-1} is attributed to C=C stretching vibration. The spectrum presents also a medium band at 722 cm^{-1} that is produced by the long-chain methylene rocking vibrations, where all of the methylene groups rock in phase, which is a characteristic of the long carbon skeleton fatty acids $–(CH_2)_n–$ [15].

3.2 Infrared spectroscopy of crude phosphate

Figure 2 shows the infrared absorption spectrum of crude natural phosphate. The strong band observed around 1047 cm^{-1} is attributed to ν_3 asymmetric stretching vibration of PO_4^{3-} phosphate anions, which broadened by shoulder band at 1084 cm^{-1} can be assigned also to ν_3 PO_4^{3-} groups [16]. The bands observed at 602 cm^{-1} can be assigned to out–of–plane bending vibration ν_4 of phosphate group (PO_4^{3-}) [17,18]. The band located at 473 cm^{-1} is attributed to the symmetrical strain mode ν_2 (PO_4^{3-}) [19]. The spectrum exhibits a less band at 970 cm^{-1}, it is attributed to symmetric stretching vibration ν_1 of phosphate PO_4^{3-} [19]. The doublet located around 1432 cm^{-1} and 1457 cm^{-1}, is associated to ν_3 (CO_3^{2-}), while the absorption band observed at 864 cm^{-1} is assigned to the ν_2 bending vibrations of the carbonate group (CO_3^{2-}) [20,21], consistent with the carbonate fluorapatite spectra previously reported by Fleet [22] and Wang *et al.* [23]. It corresponds to the out-of-plane oscillating movement of C atoms. The wavenumbers of carbonate vibrations illustrated in Figure 2 show the characteristic bands of type B carbonate-fluorapatite (CO_3^{2-} substitute PO_4^{3-} ions). Both vibration bands observed at 1616 cm^{-1} and 1637 cm^{-1} were attributed to the bending vibration of the hydroxyl (OH^-) of H–O–H [21,24-26]. The series of vibrations were observed in the 3200 cm^{-1} to 3550 cm^{-1} region could be assigned to OH group asymmetric and symmetric stretching vibrations. The bands observed in the range 2000 cm^{-1} to 2100 cm^{-1} are due to overtone of PO_4 groups bands observed in 1040 cm^{-1} to 1100 cm^{-1} region.

3.3 Experiments of phosphate flotation

3.3.1 Effect of flotation time

The flotation time is one of among important factors affecting the enrichment of the phosphate ore by the flotation process. Table 3 and Figure 3 and Figure 4 show the experimental results that were achieved at four different times of the flotation while keeping the rest of the factors constant. As observed from Table 3, the flotation time increases by 10 min for each experiment, this increase represents a remarkable effect on the P_2O_5 grade of the concentrate (sinking) and also a decrease in the float. This shows that there is reverse flotation, therefore the adsorption of the soybean oil soap collector (SOC) on the gangue particles was verified for all experiments carried out.

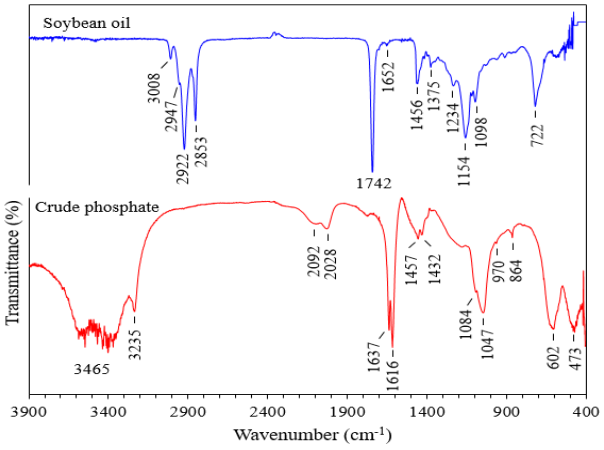

Figure 2. ATR-FTIR spectra of crude soybean oil and crude phosphate.

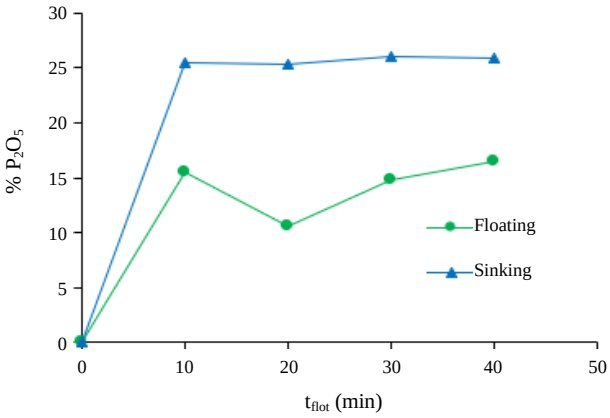

Figure 3. Variation of the % P_2O_5 of the floating and sinking as a function of flotation time (t_{flot}).

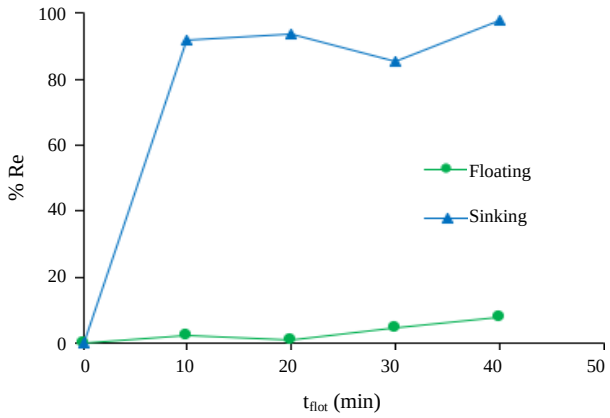

Figure 4. Variation of the recovery rate of the floating and sinking as a function of flotation time (t_{flot}).

Table 3. Variation of P_2O_5 content and recovery (Re) as a function of flotation time (t_{flot}).

$t_{flotation}$ (min)	10		20		30		40	
Samples	**Float**	**Sink**	**Float**	**Sink**	**Float**	**Sink**	**Float**	**Sink**
Yield (%)	3.7	89.0	2.8	88.4	8.3	80.8	11.7	91.8
% BPL	34.0	55.7	23.0	55.5	32.5	57.1	35.9	56.6
% P_2O_5	15.6	25.5	10.5	25.4	14.9	26.1	16.4	25.9
% Re	2.3	91.8	1.2	93.5	5.0	85.3	7.9	97.9
Separation efficiency (E)*	-	2.8	-	5.1	-	4.5	-	6.1

*(E= Recovery (%) – Yield (%))

According to the above experimental study, the P_2O_5 contents of the phosphate concentrate which are obtained in 10 min, 20 min, 30 min, and 40 min of flotation are respectively 25.5%, 25.4%, 26.1%, and 25.9%. Even if the 30 min time give a higher P_2O_5 grade (26.1%) compared to the other flotation times, on the other hand, it gave a low separation efficiency (4.5%). Consequently, the time of 20 min represent an optimal value because it gives a higher separation efficiency (5.1%) and recovery rate % Re = 93.5% with 25.4% for P_2O_5 content. From observation during experiments which showed that this time was sufficient to give a sufficient quantity of concentrate while 40 min was a long flotation time and the foam would be reduced before the end of this period.

Indeed, the flotation time of a separate particle demands mainly elementary steps as collision, attachment, and remaining on the air bubble until the slurry surface [27]. Thus, the flotation kinetics can be can written in terms of the probability between the ore particles and bubble flotation [27], this probability is given by Equation (3):

$$P_{flotation} = P_{collision} \times P_{attachment} \times P_{stay} \qquad (3)$$

where $P_{collision}$ is collision probability of a particle with an air bubble that depends on particle size, air bubble volume and solid content, while it is not affected by conditioning. $P_{attachment}$ is the probability of adhesion of the particle to the air bubble after collision, which essentially depends upon the surface physicochemical properties of the mineral, the capacity of collector absorption on the particle surface, and the time required for the hydrophobic particle to be suspended from the air bubble. P_{stay} is the probability of the particle remaining attached to the bubble along the flotation steps. Over the collision, the contact time greatly influences the production of the attachment. This time is requisite for the disjoining layer of water between particle and air bubble to thin, be disrupted and finally removed. This period is called the induction time. So, the probability of bubble particle attachment increases when the induction time decreases [28]. According to Henwood [28], the flotation time depends on $P_{collision}$ and $P_{attachment}$ which themselves depend precisely on the rate of solid and the criticisms of the solution. Consequently, the rate of solids greatly influences the float time. In this study, a very low rate of solids (6%) was applicated for all tests, this is why, the optimal flotation time was extremely long (30 min).

3.3.2 Effect of conditioning time

The results of reverse flotation for the particle size class studied as well as the yields of weight recovery of phosphate at different conditioning times are presented in Table 4. It also represents the % P_2O_5 content and recovery for the flotation products (floating and sinking). As shown in this table, the optimal conditioning time value is 10 min. Figure 5 and Figure 6 showed a remarkable increase in % P_2O_5 (26.1%) with a recovery rate 87.0% by increasing the conditioning time to reach the maximum grade (%) at 10 min. Beyond this time, there is a decrease in % P_2O_5 and also the recovery rate % Re. Indeed, this difference can be explained by the increase in the consumption of flotation reagents.

During the conditioning, Henwood, (1994) [28] showed that the adsorption of collector onto the mineral surface is done in two micro-processes. In the first step, the collector molecules diffuse out of the bulk phase, through the confined liquid film around the mineral particle to the surface of this particle. If Δr was considered as a distance travelled by the collector and Δc is the difference in concentration

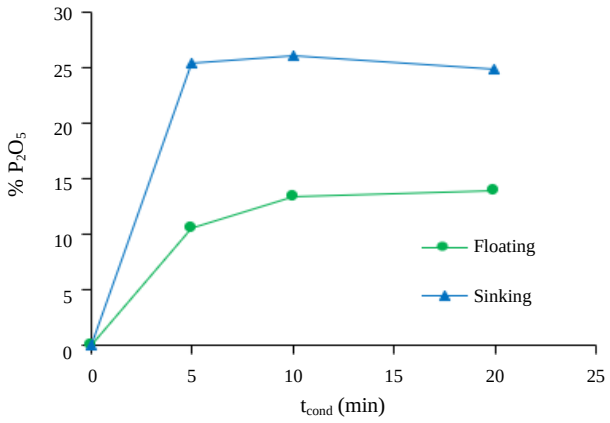

Figure 5. Variation of the % P_2O_5 of the float and sink as a function of conditioning time (t_{cond}).

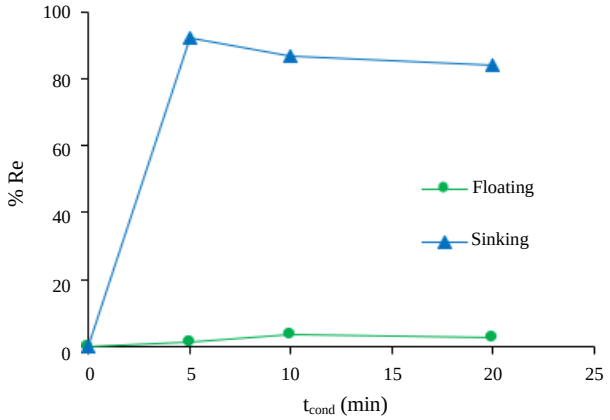

Figure 6. Variation of the sinking and floating recovery rate as a function of conditioning time (t_{cond}).

of the collector between the surface and the bulk liquid, then the rate of diffusion of the collector to the mineral surface can be increased in two ways, either by increasing the concentration of collector in the liquid or by reducing distance (for example, by increased turbulence in the flotation cell). The second step concerns affinity of water, which is determined by the energy required by the collector to shift the water at the mineral surface [28], this is affected by polarity at particles-molecules interface and the strength of bonds. This factor is largely determined by pH of media, surface chemistry and temperature. For that the conditioning time must be sufficient in order to have a good separation efficiency (Table 4). In this work, we can explain the long conditioning time by the low solid content which is 6%, thus a long path from collector to particle (Δr). Therefore, it is necessary to add additional time to diffuse and adsorb the collector to the surface of the mineral particles.

3.3.3 Effect of pH

The pH factor plays an essential role in the flotation of phosphates; it allows the separation of undesirable minerals from desirable ones in direct or reverse flotation. Indeed, the pH of the solution determines the degree of ionization and hydrolysis of the collector used; this solution character favors or prevents the adsorption of the collector at the different ionized solid/liquid interfaces, which leads to a greater or lesser selectivity of the flotation [29].

Various experiments were studied by varying the pH values from 4.05 to 10.05 as shown in Table 5. While the other flotation conditions were fixed at 125 µm to 90 µm particle size, 1 g of soybean oil soap collector, 20 min flotation time, 10 min conditioning time, 0.17 L· min^{-1} air superficial velocity and 800 rpm at about 25°C. Table 5 and Figure 7 and Figure 8 demonstrate the effect of pH of the pulp in the presence of soybean oil soap collector and using phosphoric acid as pH regulator. It can be seen that the separation of flotation efficiency increased with decreasing pH values from pH 5. It is observed that the using of soybean oil soap as a collector showed a better result working and high recovery 94.5% in pH 4.05 where it gives a high closer value of grade 29.0%.

Usually, fatty acid collectors and their soaps are used for phosphate ores flotation which contain a silicates percentage around 20% to 25% in the feed because at a basic pH they have a negatively charged carboxylate group which can act as a repellent to the silicate minerals, and again in an acidic pH fatty acid can float carbonates instead of phosphate [30]. In that case, soybean oil collector would adsorb selectively to carbonate particles rather than to phosphate particles. The depression of apatite is done at pH of the pulp below 4.5 during an apatite anionic flotation without the addition of any other phosphate depressant [31].

During a froth flotation, Prasad *et al*. [32] showed that the oleic acid, which is anionic collector, acts as a depressant for apatite and a floater for calcium carbonates. The explanation of these phenomena will be as follows: firstly, when the phosphoric acid used as pH regulator, the action of the acid on the apatite gives rise to the following reactions that producing soluble calcium-phosphate compound forms, $CaHPO_4$, on the surface of apatite mineral [33], which prevents the collector ions from attaching to the surface of the apatite mineral. As shown in the Equations (4) and (5):

$$Ca_5(PO_4)_3(OH)(s) + 2\,PO_4^{3-} + 6\,H^+ \Leftrightarrow 5\,CaHPO_4(s) + H_2O \quad (4)$$

$$CaHPO_4(s) \Leftrightarrow CaHPO_4\,(aq) \quad (5)$$

Secondly, the attack of $CaCO_3$ by phosphoric acid releases Ca^{2+} ions on the surface of the calcite as shown by the following reaction (Equation (6)):

$$2\,H^+ + CaCO_3 \Leftrightarrow Ca^{2+} + H_2CO_3 \quad (6)$$

Then, the formation of the highly insoluble $Ca_3(PO_4)_2$ by a reaction of PO_4^{3-} and Ca^{2+} ions according to the Equation (7):

$$3\,Ca^{2+} + 2\,PO_4^{3-} \Leftrightarrow Ca_3(PO_4)_2\,(s) \quad (7)$$

Finally, the surface of the calcite becomes a more stable phase leading to the formation of Ca-oleate on the surface after adding an oleate-based collector. On the other hand, the surface of apatite contains a more soluble phase ($CaHPO_4$ (aq)) than that of calcite, which can reduce the adsorption of oleic acid that is one of main oil soybean constituent [34].

Table 4. Variation of P_2O_5 content and recovery (Re) as a function of conditioning time (t_{cond}).

$T_{conditioning}$ (min)	5		10		20	
Samples	**Float**	**Sink**	**Float**	**Sink**	**Float**	**Sink**
Yield (%)	2.8	88.4	6.2	82.4	4.3	83.8
% BPL	23.0	55.5	29.4	57.1	30.5	54.3
% P_2O_5	10.5	25.4	13.4	26.1	13.9	24.8
% Re	1.2	92.4	3.4	87.0	2.4	84.1
Separation efficiency (E)*	-	4.0	-	4.6	-	0.3

* (E= Recovery (%) – Yield (%))

Table 5. Variation of P_2O_5 content and recovery rate (Re) as a function of pH value.

pH	4.05		5.50		7.01		8.60		10.05	
Samples	**Float**	**Sink**	**Float**	**Sink**	**Float**	**Sink**	**Float**	**Sink**	**Float**	**Sink**
Yield (%)	8.6	84.5	4.2	83.0	4.2	86.9	6.2	82.4	3.0	83.2
% BPL	21.4	63.3	19.1	60.5	21.5	59.3	29.4	57.1	26.0	56.9
% P_2O_5	9.8	29.0	8.7	27.7	9.8	27.2	13.4	26.1	11.9	26.0
% Re	3.3	94.5	1.4	88.6	1.6	91.3	3.4	87.0	1.4	83.5
Separation efficiency (E)*	-	10.1	-	5.6	-	4.4	-	4.6	-	0.3

*(E= Recovery (%) – Yield (%))

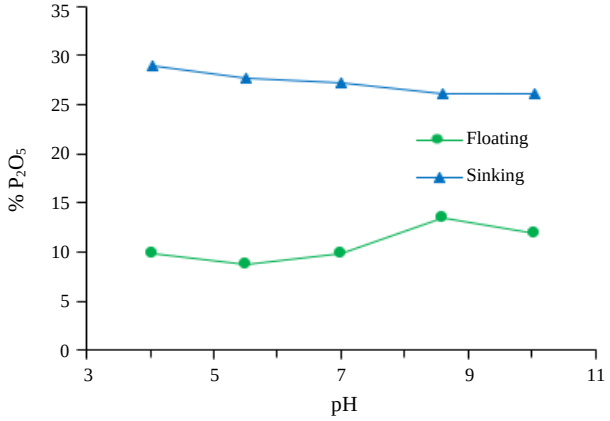

Figure 7. Variation of the % P_2O_5 of the sinking and floating as a function of the pH.

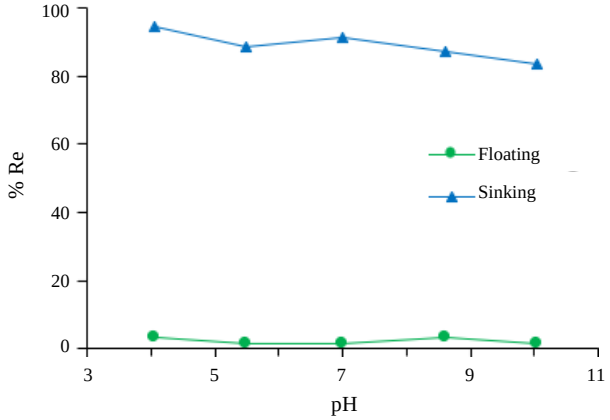

Figure 8. Variation of the recovery rate of the sinking and floating as a function of the pH.

4. Analysis of the flotation products

4.1 FTIR spectrometry analysis

Figure 9 shows a FTIR spectra of the floating, sinking and crude sample in order to apprehend the evolution of the mineral phases depressed and floated related to the optimal parameters (pH = 4.05; conditioning time: 10 min; flotation time: 20 min). It can be seen that these spectra clearly show the most bands allocated to the phosphatic elements observed previously and carbonated apatite. As shown in Figure 9, the appearance and disappearance of bands on the infrared spectra of the flotation products is observed. To analyse the presence of carbonate in the flotation products, a focus on the 650 cm^{-1} to 900 cm^{-1} region shown in Figure 9 indicates the appearance of a new band at 876 cm^{-1} just in the float which corresponds to calcite and dolomite carbonates with the presence of bands at 727 cm^{-1} and 711 cm^{-1} corresponding to dolomite and calcite carbonates respectively. Also, the band at 864 cm^{-1} of apatite carbonates is much more intense in the sinking then in floating [35], which this carbonate type is part of the phosphate bulk. This qualitative FTIR study confirmed the results obtained of the grade and recovery rate of P_2O_5 during the phosphate ores flotation, as well as the SOC collector is selective for the carbonate gangue and therefore the flotation was reverse.

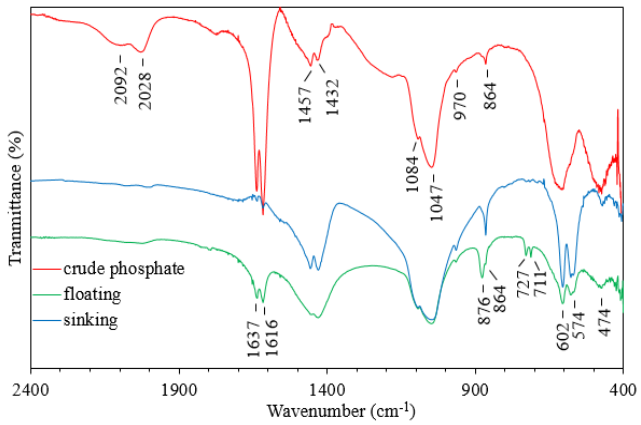

Figure 9. FTIR spectra of the flotation products obtained with the studied optimal parameters.

El Feki *et al*. [36] have described the low intensity carbonates bands around 870 cm^{-1} and around 716 cm^{-1} to 718 cm^{-1} and the reasons of the splitting into two bands for carbonates in apatite: this is bounded to different surrounding of carbonates ions in apatite lattice. A similar phenomenon was observed between calcite (calcium surrounding) and dolomite (calcium/magnesium surrounding). They thus described in apatite two types of carbonates sites: anionic monovalent site that named the A type and phosphate trivalent site that named the B type. Rey *et al*. [37] are also using these bands to study teeth enamel evolution during growing.

According to the sinking spectrum in Figure 9, the complete disappearance of the characteristic bands of water located at 1616 cm^{-1} and 1637 cm^{-1} was observed which remain in the spectrum of the floating. This can be bounded to the constitution water in different mineralogical forms of the gangue as $CaCO_3.xH_2O$, $SiO_2.xH_2O$, $CaSO_4.xH_2O$ passed to the floating during the flotation process. In most cases, the intensity of the characteristic peaks of phosphatic groups is clearly more remarkable in the flowing than in the floating. Two low peaks observed about 2922 cm^{-1} to and 2853 cm^{-1} corresponding to the symmetric and asymmetric -C-H (CH_2) stretching vibrations of collector adsorbed on the mineral particles.

4.2 X-ray diffraction analysis

X-ray diffraction and mineralogical analysis showed that raw phosphate was present as carbonate-fluorapatite which is also called francolite [38,39]. While the main gangue minerals, in decreasing order, were carbonates (dolomite and calcite) and free quartz as illustrated in Figure 10. Figure 11 shows the X-ray diffractograms of the floating, sinking and crude ore samples in order to understand the evolution of the depressed and floated mineral phases after all flotation steps with optimum parameters (pH = 4.05; conditioning time: 10 min; flotation time: 20 min). From a concrete analysis of this diffractograms, there are changes between the floating and the sinking at the characteristic peaks of dolomite, calcite and quartz. for the sinking diffractogram, there is a notable decrease at the level of the two characteristic peaks of the calcite as indicated in Figure 11 by the two following signs (∗, °). There is still a perfect elimination of dolomite that is represented by a peak signed by (◊). Thus, let's not

forget a remarkable change at the level of the peak signed by (•) which represents the quartz phase. In contrary, for the floating diffractogram, all the peaks mentioned above led to a remarkable increase especially the characteristic peak of calcite. Consequently, all these outcomes confirm the results found by the analysis of the FTIR.

5. Flowchart of natural froth flotation results.

As stated by the optimum conditions of the natural flotation processes, a schematic diagram of the beneficiation was made for the removal of gangue with a froth flotation. The flowchart and optimal parameters of the flotation were represented in Figure 12.

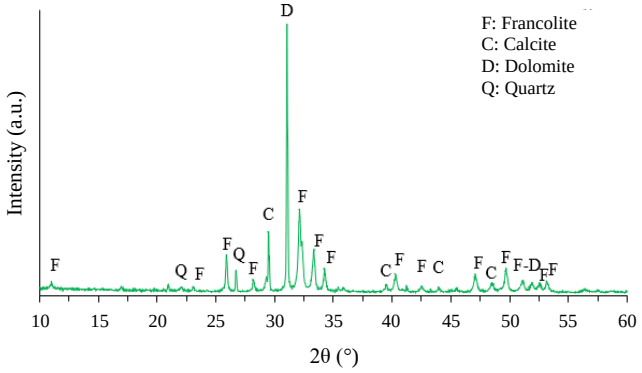

Figure 10. XRD diffractogram of raw phosphate sample.

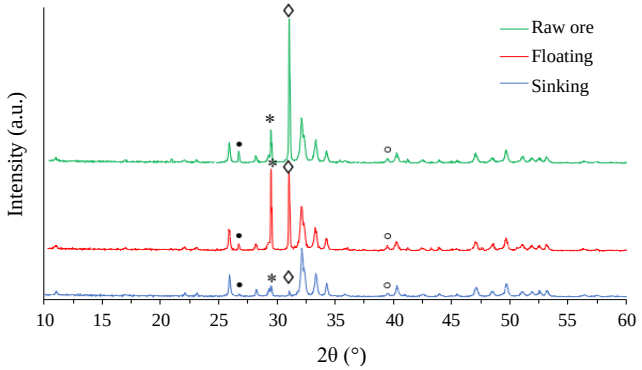

Figure 11. XRD diffractogram of phosphate flotation product (sinking and floating).

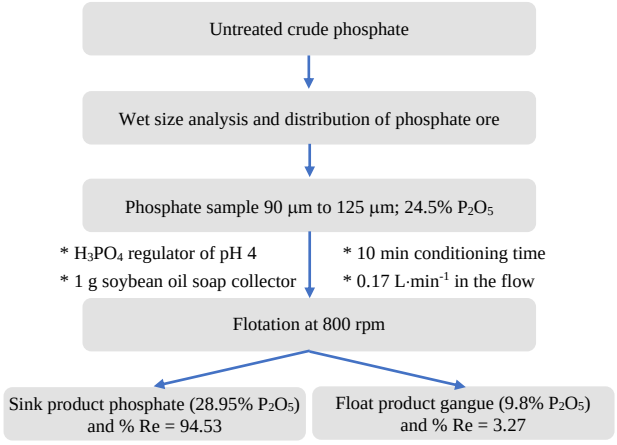

Figure 12. Flowchart of natural phosphate flotation process.

6. Conclusion

According to the experimental results found in this work, the following conclusions can be drawn: the direct bioflotation tests using saponified soybean oil indicate that this oil can be used satisfactorily as a collector flotation for apatite. Soybean oil showed better results working in pH 4 in the presence of a regulator of pH as H_3PO_4. Based on the above optimal conditions, a phosphate concentrate was obtained 29.0% P_2O_5 with a recovery of 94.5%, demonstrating the efficiency of the method. The analysis of flotation products by FTIR, XRD and UV-VIS techniques confirmed that the gangue minerals were separated from the phosphate ores by reverse flotation.

Acknowledgments

The authors thank all who assisted in conducting this work.

References

[1] Q. Cao, J. Cheng, S. Wen, C. Li, S. Bai, and D. Liu, "A mixed collector system for phosphate flotation," *Minerals Engineering*, vol. 78, pp. 114-121, 2015.

[2] M. Gharabaghi, M. Noaparast, and M. Irannajad, "Selective leaching kinetics of low-grade calcareous phosphate ore in acetic acid," *Hydrometallurgy*, vol. 95, no. 3-4, pp. 341-345, 2009.

[3] A. Z. M. Abouzeid, "Physical and thermal treatment of phosphate ores - An overview," *International Journal of Mineral Processing*, vol. 85, no. 4, pp. 59-84, 2008.

[4] S. Khoshjavan, and B. Rezai, "Beneficiation of refractory rock phosphate by calcination and flotation," *Mining, Metallurgy & Exploration*, vol. 28, no. 4, pp. 187-192, 2011.

[5] D. A. Elgillani, and A. Z. M. Abouzeid, "Flotation of carbonates from phosphate ores in acidic media," *International Journal of Mineral Processing*, vol. 38, no. 3-4, pp. 235-256, 1993.

[6] A. Z. M. Abouzeid, A. T. Negm, and D. A. Elgillani, "Upgrading of calcareous phosphate ores by flotation: Effect of ore characteristics," *International Journal of Mineral Processing*, vol. 90, no. 1-4, pp. 81-89, 2009.

[7] S. A. Abouel-enein, H. S. Gado, A. A. El-shennawy, A. M. Masoud, and A. A. Ahmed, "Phosphate Froth Flotation Using Sesame Oil as a Collector," *Journal of Basic and Environmental Sciences*, vol. 7, pp. 106-123, 2020.

[8] C. Owusu, K. Quast, and J. Addai-Mensah, "The use of canola oil as an environmentally friendly flotation collector in sulphide mineral processing," *Minerals Engineering*, vol. 98, pp. 127-136, 2016.

[9] E. P. Santos, A. J. B. Dutra, and J. F. Oliveira, "The effect of jojoba oil on the surface properties of calcite and apatite aiming at their selective flotation," *International Journal of Mineral Processing*, vol. 143**,** pp. 34-38, 2015.

[10] Y. Ruan, Z. Zhang, H. Luo, C. Xiao, F. Zhou, and R. Chi, "Ambient temperature flotation of sedimentary phosphate ore using cottonseed oil as a collector," *Minerals*, vol. 7, no. 5, pp. 1-14, 2017.

[11] P. Zhang, and R. Snow, "Studies of anionic reagents for phosphate beneficiation," *Mining, Metallurgy & Exploration*, vol. 26, pp. 65-73, 2009.

[12] T. E. Clemente, and E. B. Cahoon, "Soybean Oil: Genetic Approaches for Modification of Functionality and Total Content," *Plant Physiology*, vol. 151, no. 3, pp. 1030-1040, 2009.

[13] J. Kuligowski, G. Quintás, F. A. Esteve-Turrillas, S. Garrigues, and M. de la Guardia, "On-line gel permeation chromatography-attenuated total reflectance-Fourier transform infrared determination of lecithin and soybean oil in dietary supplements," *Journal of Chromatography A*, vol. 1185, no. 1, pp. 71-77, 2008.

[14] M. J. Lerma-García, G. Ramis-Ramos, J. M. Herrero-Martínez, and E. F. Simó-Alfonso, "Authentication of extra virgin olive oils by Fourier-transform infrared spectroscopy," *Food Chemistry*, vol. 118, no. 1, pp. 78-83, 2010.

[15] J. V. Kadamne, V. P. Jain, M. Saleh, and A. Proctor, "Measurement of Conjugated Linoleic Acid (CLA) in CLA-Rich Soy Oil by Attenuated Total Reflectance-Fourier Transform Infrared Spectroscopy (ATR-FTIR)," *Journal of Agricultural and Food Chemistry*, vol. 57, pp. 10483-10488, 2009.

[16] T. Furuzono, D. Walsh, K. Sato, K. Sonoda, and J. Tanaka, "Effect of reaction temperature on the morphology and size of hydroxyapatite nanoparticles in an emulsion system," *Journal of Materials Science Letters*, vol. 20, no. 2, pp. 111-114, 2001.

[17] M. Dakkach, A. Atlamsani, and S. Sebti, "Natural phosphate modified by vanadium: A new catalyst for oxidation of cycloalkanones and α-ketols with oxygen molecular," *Comptes Rendus Chimie*, vol. 15, no. 6, pp. 482-492, 2012.

[18] M. Sadiq, M. Abdennouri, N. Barka, M. Baalala, C. Lamonier, and M. Bensitel, "Influence of the Crystal Phase of Magnesium Phosphates Catalysts on the Skeletal Isomerization of 3,3-dimethylbut-1-ene," *Canadian Chemical Transactions*, vol. 3, no. 2, pp. 225-233, 2015.

[19] C. Drouet, "Apatite formation: Why it may not work as planned, and how to conclusively identify apatite compounds," *BioMed Research International*, vol. 2013, no. 4, pp. 1-12, 2013.

[20] E. M. Zahrani, and M. H. Fathi, "The effect of high-energy ball milling parameters on the preparation and characterization of fluorapatite nanocrystalline powder," *Ceramics International*, vol. 35, pp. 2311-2323, 2009.

[21] I. Nikcevic, V. Jokanovic, M. Mitric, Z. Nedic, D. Makovec, and D. Uskokovic, "Mechanochemical synthesis of nano-structured fluorapatite/fluorhydroxyapatite and carbonated fluorapatite/fluorhydroxyapatite," *Journal of Solid State Chemistry*, vol. 177, pp. 2565-2574, 2004.

[22] M. E. Fleet, "Infrared spectra of carbonate apatites: ν_2-Region bands," *Biomaterials*, vol. 30, no. 8, pp. 1473-1481, 2009.

[23] M. Wang, R. Qian, M. Bao, C. Gu, and P. Zhu, "Raman, FT-IR and XRD study of bovine bone mineral and carbonated apatites with different carbonate levels," *Materials Letters*, vol. 210, pp. 203-206, 2018.

[24] R. Yous, F. Mohellebi, H. Cherifi, and A. Amrane, "Competitive biosorption of heavy metals from aqueous solutions onto Streptomyces rimosus," *Korean Journal of Chemical Engineering*, vol. 35, pp. 890-899, 2018.

[25] R. D. Aines, and G. R. Rossman, "Water in Minerals? A Peak in the Infrared," *Journal of Geophysical Research: Solid Earth*, vol. 89, no. B6, pp. 4059-4071, 1984.

[26] K. Boughzala, and K. Bouzouita, "Synthesis and characterization of strontium–calcium–lanthanum apatites $Sr_{7-x}Ca_xLa_3(PO_4)_3(SiO_4)_3F_2$ $0 \leq x \leq 2$," *Comptes Rendus Chimie*, vol. 18, no. 8, pp. 858-866, 2015.

[27] C. E. Jordan, and D. R. Spears, "Evaluation of a turbulent flow model for fine-bubble and fine-particle flotation," *Mining, Metallurgy & Exploration*, vol. 7, pp. 65-73, 1990.

[28] D. Henwood, "*The effect of conditioning on froth flotation*," Dissertations, cape town University, July 1994.

[29] S. R. Rao, "*Surface Chemistry of Froth Flotation*," Volume 1: Fundamentals New York, 2004.

[30] L. Zhang, "*Enhanced phosphate flotation using novel depressants*," Theses and Dissertations-Mining Engineering 10, Kentucky University, 2013.

[31] Y. Ruan, Z. Zhang, H. Luo, C. Xiao, F. Zhou, and R. Chi, "Effects of metal ions on the flotation of apatite, dolomite and quartz," *Minerals*, vol. 8, no. 4, pp. 1-12, 2018.

[32] M. Prasad, A. K. Majumder, and T. C. Rao, "Reverse flotation of sedimentary calcareous/dolomitic rock phosphate ore - an overview," *Mining, Metallurgy & Exploration*, vol. 17, no. 1, pp. 49-55, 2000.

[33] X. Shao, C. L. Jiang, and B. K. Parekh, "Enhanced flotation separation of phosphate and dolomite using a new amphoteric collector," *Mining, Metallurgy & Exploration*, vol. 15, pp. 11-14, 1998.

[34] Z. E. Öztin, "*Parametric studies on cell flotation of mazidağı phosphate rock*," PhD Thesis, Middle East Technical University, September 2003.

[35] I. Birken, M. Bertucci, J. Chappelin, and E. Jorda, "Quantification of impurities, including carbonates speciation for phosphates beneficiation by flotation," *Procedia Engineering*, vol. 138, pp. 72-84, 2016.

[36] H. El Feki, C. Rey, and M. Vignoles, "Carbonate Ions in Apatites: Infrared Investigations in the ν_4 CO_3 Domain," *Calcified Tissue International*, vol. 49, pp. 269-274, 1991.

[37] C. Rey, V. Renugopalakrishnan, M Shimizu, B. Collins, and M. Glimcher, "A resolution-enhanced Fourier transform Infrared spectroscopy of the environment of the CO_3^{2-} ion in the mineral phase of enamel during its formation and maturation," *Calcified Tissue International*, vol. 49, pp. 259-268, 1991.

[38] A. Kenzour, H. Belhouchet, M. Kolli, S. Djouallah, and D. Kherifi, S. Ramesh, "Sintering behavior of anorthite-based composite ceramics produced from natural phosphate and kaolin," *Ceramics International*, vol. 45, pp. 20258-20265, 2019.

[39] W. Gallala, F. Herchi, I. Ben Ali, L. Abbassi, M. E. Gaied, and M. Montacer, "Beneficiation of Phosphate Solid Coarse Waste from Redayef (Gafsa Mining Basin) by Grinding and Flotation Techniques," *Procedia Engineering*, vol. 138, pp. 85-94, 2016.